Oxidation of Step Edges on Si(001)-$c(4 \times 2)$

C.-H. Chung,[1] H. W. Yeom,[1,2] B. D. Yu,[3] and I.-W. Lyo[1,*]

[1]*Institute of Physics and Applied Physics, Yonsei University, Seoul 120-749, Republic of Korea*
[2]*Center for Atomic Wires and Layers, Yonsei University, Seoul 120-749, Republic of Korea*
[3]*Department of Physics, University of Seoul, Seoul 130-743, Republic of Korea*

(Received 19 October 2005; published 19 July 2006)

The initial oxidation process of the ultraclean Si(001)-$c(4 \times 2)$ surface is studied using scanning tunneling microscopy at low temperature. At the early stage of oxygen adsorption, reactions with Si atoms at S_B steps are dominant over those at terraces by more than 2 orders of magnitude, and they proceed in two distinct stages to high oxidation states. Guided by the *ab initio* calculations, the oxidation structures at each stage are proposed. The extreme reactivity of the step edge is due to the presence of rebonded adatoms with dangling bonds and weak rebonds, and their proximity allows the formation of -Si-O- chain structures along the step edge, unlike those on the Si(111) surface.

DOI: 10.1103/PhysRevLett.97.036103 PACS numbers: 81.65.Mq, 68.37.Ef, 68.43.Bc, 68.43.Fg

Silicon dioxide may arguably be the most studied oxide material to date, thanks to its undisputable technological importance. Not surprisingly, the initial oxidation process on Si surfaces has long been a source of technological as well as fundamental interest [1–10].

Nevertheless, there have been many issues still left unresolved, particularly those concerning the early stage of oxidation such as the existence of precursor states [11,12], initial oxide growth modes [13], and reaction pathways [14]. While models on oxygen adsorption on Si(001) to date have almost exclusively focused on buckled Si dimers at the terrace [1,10,14–16], a detailed understanding of the initial oxidation process of the surface had always been complicated by overwhelming inhomogeneity due to high density defects [8].

Not surprisingly, the oxidation of intrinsic nanostructures such as step edges has attracted little attention until now. Of two native step structures on Si(001), the S_B step edge shares more similarity with the adatoms on Si(111)-(7×7) than the π-bonded dimers on Si(001), by having a rebonded Si adatom (RSA) with a dangling bond (DB) and three backbonds [17]. In addition, these one-dimensionally aligned RSA's are buckled alternately and separated by about half the distance between adatoms on Si(111). Thus, the study of oxidation at step edges may not only provide important insights into the oxidation mechanism of the surface through the direct comparison of the reactions at two heterostructures but also raise a possibility of forming a novel Si oxide structure.

In this Letter, we report on the investigation of the initial oxidation on the Si(001)-$c(4 \times 2)$ surface at a low temperature (80 K), with a particular focus on the step edges. A low temperature scanning tunneling microscope (STM) was used, as its atomic resolution capability is ideally suited for this study. In order to obtain defect-free surfaces, exhaustive care was exercised until typically no C-type defects and a very low density of A- and B-type defects ($<0.5\%$) remained on the surface. By comparing the signatures of oxygen adsorption with *ab initio* calculations, we were able to elicit the oxygen reacted S_B step structures. The results suggest far reaching implications of the step edge to the oxidation process of the pristine Si(001) surface, as well as the formation of exotic linear Si oxide chains not observed before.

Experiments were performed at the base pressure less than 3×10^{-11} mbar. In order to prepare the ultraclean Si(001) surface, the n-type, 1 Ω cm, sample was outgassed at $\sim$670 K over a few days and annealed to $\sim$1270 K for 1 h [18], while keeping the pressure below 6×10^{-11} mbar. The sample was then flashed to $\sim$1470 K at less than 4×10^{-11} mbar. Liquid nitrogen traps were used to reduce residual water molecules, a source of C-type defects [19]. Oxygen dosing was performed by backfilling the chamber.

Figure 1 shows typical, atomically resolved STM images of the S_B steps on the Si(001)-$c(4 \times 2)$ surfaces at low temperature at each step of oxygen dosing. The pristine steps are characterized by, as shown in Fig. 1(b), the bright protrusions at S_B step edges prominent at the empty state images [20]. After the exposure to the oxygen dose of 0.12 L, the filled state images indicated little change, as the comparison of STM images 1(a) and 1(c) demonstrates. However, dramatic changes were found in the empty state. The bright protrusions disappeared in proportion to the oxygen dose, as shown in Fig. 1(d).

At a higher dose of 0.3 L, a new feature in the form of dark trenches emerged, as shown in Figs. 1(e) and 1(f). This dark trench is oriented parallel to the S_B step edge and is located between the end of the dimer rows at the upper terrace and the first dimer row at the lower terrace. Unlike the oxygen reaction at terraces [7,8,10], no ejection of substrate materials was found during the oxidation of the step edges. Also, no signature of oxidation at S_A step edges was found, in agreement with the previous report [8]. Thus, these data indicate that the step-edge oxidation proceeds in two distinct stages, which will be characterized in detail below.

At the same time, Fig. 1 clearly demonstrates that there is little reaction occurring at terraces during step oxidation.

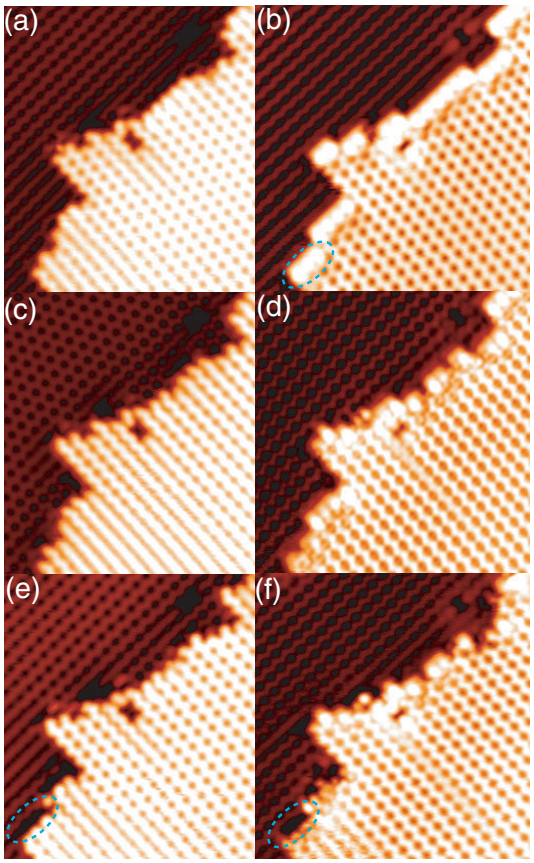

FIG. 1 (color online). Sequential STM images of filled states of −2.5 V [(a), (c), and (e)] and empty states of +1.2 V [(b), (d), and (f)] of Si(001)-$c(4 \times 2)$ at 80 K. The oxygen dose was (a)–(b) 0, (c)–(d) 0.12, and (d)–(f) 0.30 L. Dotted ellipses mark the same area with (b) bright protrusions and (e)–(f) dark trenches.

The reaction ratio of the bright protrusion sites along S_B steps at the exposure of oxygen 0.12 L was ~39%, while that of the bare dimers at the terraces was ~0.3%, leading to the ratio of ~130. The oxidation at terraces followed only after the early saturation of oxidation at S_B steps, similar to the previous STM results at room temperature [7].

In order to gain an understanding of the oxidation structures and reaction pathways at step edges, we performed density functional theory (DFT) calculations within the generalized gradient approximation using the VASP [21] and ultrasoft pseudopotentials [22]. The single-layer Si(001) steps were simulated by using a repeating slab structure consisting of six Si layers with a H-terminated bottom surface and an 8-Å-thick vacuum region as shown in Fig. 2. A vicinal (1 1 19) surface with an alternating sequence of S_A and S_B steps was used to examine the relative adsorption energies of oxygen atoms at the step edges. A cutoff energy of 260 eV and a uniform mesh of 4 **k** points in the surface Brillouin zone of the lateral unit cell were used. All atoms were relaxed in the slab except for the bottom-most Si and H atoms. The geometry optimization was terminated when the remaining forces were smaller than 0.02 eV/Å.

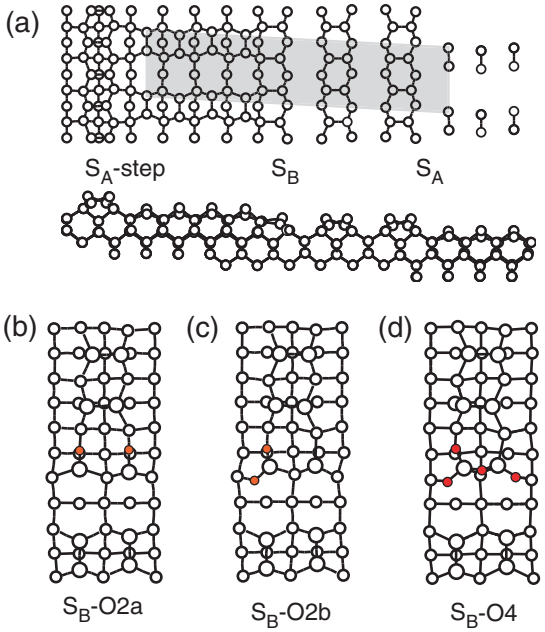

FIG. 2 (color online). (a) Top and side views of the stepped Si(001)-$c(4 \times 2)$ surface. The gray box denotes the unit cell used in the calculation. Perspective views of the possible stable structures of the rebonded S_B steps reacted with (b)–(c) two and (d) four oxygen atoms per unit cell. Open and dark (red) circles denote Si and oxygen atoms, respectively, with larger open circles in (b)–(d) denoting surface Si atoms.

Figure 2(a) shows the stepped Si(001)-$c(4 \times 2)$ structure used in our calculation. A S_B step is formed by having Si atoms rebond to the second layer Si atoms at the upper terrace, thus reducing the DB density. These RSA's buckle alternately up and down to further reduce the energy. Among the several possible step oxidation structures with two oxygen atoms per unit cell considered, only two structures were found stable: S_B-O2a [Fig. 2(b)] and S_B-O2b [Fig. 2(c)], where the number in each notation denotes that of oxygen atoms in the unit cell.

In the S_B-O2a structure, a dissociated oxygen molecule would insert each oxygen atom into a bridge rebond that connects a RSA and the second layer Si atom bonded to the step-edge dimer. In the S_B-O2b structure, two oxygen atoms react with a single down RSA. One oxygen atom is located at the bridge rebond, and the other at the backbond of the same RSA. To determine the relative stability of the oxidation structures, the adsorption energy was calculated per oxygen atom [23]. While the S_B-O2a structure is favored over a Si dimer on a terrace with an oxygen atom in a backbond [14], by 0.36 eV per oxygen atom, S_B-O2b structure is slightly more favored by 0.06 eV per adatom over the S_B-O2a structure.

Higher oxidation structures including additional oxygen atoms were also considered. The adsorption energy calculations showed that the high oxidation structures were located at the S_B step and were more stable than the low oxidation structures S_B-O2a and -O2b. One such represen-

tative example S_B-O4 is shown in Fig. 2(d). This is the energetically most stable one among the structures with four oxygen atoms (two molecules reacted) per unit cell, as well as the most dynamically probable structure to follow S_B-O2b, when an additional oxygen molecule is adsorbed. Remarkably, all high oxidation structures share an unusual common feature: the formation of -Si-O- chain structures along the S_B step edge by bridging two neighboring RSA's through an oxygen atom, along with the consequent elimination of their DB's, as depicted in Fig. 2(d). This formation elicits a chainlike oxide structure never before observed. Our calculation shows that the adsorption energy is lowered by 0.22 eV per oxygen adatom relative to the S_B-O2a structure [23].

In order to determine the structures of reaction products, a comparison was made between the high resolution STM images and the corresponding theoretical simulations based on the oxygen reacted S_B step structures discussed above. In the STM images of the clean S_B step, as shown in Fig. 3(a), are two distinctive step-edge features. In particular, the inset in Fig. 3(a) shows these well-resolved features: circular bright protrusions located over the step-edge dimers and faint bean-shaped protrusions (pointed out by an arrowhead) attributed to DB's of the RSA's [20]. Both protrusions appeared symmetric at RT as well as at 77 K. These features are clearly reproduced in the simulated images shown in Fig. 3(d).

As oxygen molecules were introduced, bean-shaped protrusions disappeared and, simultaneously, circular bright protrusions split into two lesser symmetric ones separated by a dark node, as indicated by an arrowhead in Fig. 3(b). A few more examples of this are found in the inset as well. The dark node corresponds to the middle between the RSA's of the same dimer row.

These behaviors are successfully reproduced in the simulated images of both S_B-O2a and S_B-O2b structures as shown in Figs. 3(e) and 3(f), respectively. Unreacted RSA sites in Fig. 3(f) appear brighter than reacted ones due to the presence of the DB states near E_F. The splitting of the outermost dimer and the presence of the dark node in the middle, as marked by an arrowhead in Fig. 3(f), are also well replicated in both oxidated structures. A close inspection of images shows that the presence of the oxygen atom in the bridge rebond is the predominant factor in quenching the bean-shaped protrusions. Thus, we argue that the structure produced by a single molecular oxygen is S_B-O2b, because not only is it more energetically favored over S_B-O2a, but also the latter has to overcome the large spacing between two bridge rebonds for the reaction to take place.

On the other hand, the emergence of the dark trenches at the higher coverage cannot be explained by the oxidation of bridge rebonds alone. In particular, the splitting of circular bright protrusions located on top of the outermost dimers and its associated dark node all but disappeared in the STM images [Fig. 3(c)]. The outermost dimers now appear buckled, as if they had turned *normal*, resembling

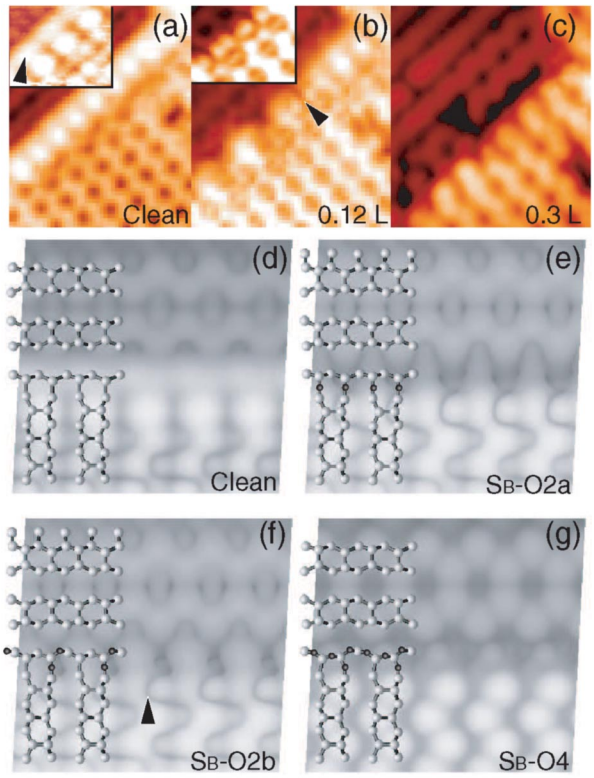

FIG. 3 (color online). The comparison of (a)–(c) the STM images and (d)–(g) the simulated ones with the ball models of the corresponding stable structures overlaid, where the bright and dark balls are Si and oxygen atoms, respectively. Images (a), (b), and (c) were over the same area in oxygen doses of 0, 0.12, and 0.3 L at the sample biases of +1.2, +1.2, and −2.5 V, respectively. The insets in (a) and (b) show high resolution images. In comparison, (d)–(g) are the simulated STM images of the clean, S_B-O2a, -O2b, and -O4 structures with the nominal applied voltage of +0.5, +0.5, +0.5, and −2.0 V, respectively. In each image, the upper half corresponds to the lower terrace.

inner ones. In comparison, simulated images in Fig. 3(e) and 3(f) do not show such features.

Both the appearance of the dark trenches and the return to *normal* dimers of the outermost ones were found in the simulated images of high oxidation structures beyond a single oxygen molecular reaction per unit cell, as shown in Fig. 3(g). The agreement indicates that the dark trench essentially represents higher oxidation states, where an oxygen atom bridges a RSA to a neighboring RSA. The formation of the RSA-O-RSA bonds eliminates the local density of states at RSA's, or DB's, and thus produce the dark trench. In short, the initial oxidation at the step edge is essentially a two-step process, namely, sequential oxidation of the bridge rebonds followed by the DB's of the RSA's.

As described earlier, RSA's at a S_B step appear structurally analogous to adatoms on Si(111)-7 × 7, having one DB and three backbonds with similar bond angles. On the Si(111) surface, the presence of molecularly chemisorbed oxygen species was reported [11,24,25]. However, our

findings argue, on two accounts, against the existence of such molecular species at the step edge at the early stage of the oxidation: (i) excellent agreement between the STM images and calculations and (ii) the weakness of the rebonds. Our calculation shows that bridge rebonds, in particular, are significantly elongated over the bulk Si bonds by as much as 0.2 Å. The RSA-O-RSA bond formation channel is not likely to support precursor states, because of the absence of Si-Si bond breaking associated with the decay and the large structural degree of freedom enjoyed by RSA's.

In addition, our finding of the difference by 2 orders of magnitude in the site selectivity of oxygen molecules for RSA's over Si dimers on a terrace has broad implications to an understanding of the oxidation of the Si(001) surface. Taken together with the observations that a typical width of terraces in our surface is 50 nm and that reaction products show no mobility at 78 K, our finding implies the existence of mobile molecular species at the surface, with a mean free path no less than 25 nm. Alternative chemisorption mechanisms would have exhibited spatially isotropic distributions of reaction sites, possibly with local anisotropy typified by a denuded zone, thus indicating a short-range interaction. However, no such distributions were found in our data. The existence of such species is supported by a molecular beam study on oxygen adsorption on Si(001) [26], as well as works by ultraviolet photoelectron spectroscopy [27] and photon-stimulated desorption [12]. The existence of such long-lived mobile species may seem at odds with the *barrierless* oxidation model proposed for the surface [14]. However, a recent calculation [28] suggests that incoming triplet oxygen molecules chemisorb barrierless only under a very stringent geometric configuration. Such a strong steric effect may explain the long mean free path and the overwhelming preference for the step-edge sites.

In conclusion, we investigated the initial oxidation process on the ultraclean Si(001)-$c(4 \times 2)$ surface at low temperature using STM and DFT calculations. At the very early stage of oxygen adsorption, dangling bonds of RSA's reacted first. The defect-free surface preparation yielded the site selectivity of oxygen molecules for RSA's over those on terraces higher by more than 2 orders. The oxidation of S_B step structures proceeded in two steps to high oxidation states. Through the comparison with STM images and the *ab initio* calculations, the stable oxidation structures at each stage are proposed. Our study not only reveals the formation of unique -Si-O- chain structures at S_B steps but also provides deep insights into the oxidation mechanism of the Si surface.

The authors are grateful to acknowledge support by MOCIE through the National R&D Project for Nano Science and Technology and in part by KOSEF through NCRC for Nano-Medical Technology. H. W. Y. and B. D. Y. are supported by the MOST through CRi program and MOCIE through the National Research Program for the 0.1 Terabit Non-Volatile Memory Development, respectively.

*Electronic address: lyo@yonsei.ac.kr

[1] T. Engel, Surf. Sci. Rep. **18**, 93 (1993), and references therein.
[2] I.-W. Lyo, P. Avouris, B. Schubert, and R. Hoffmann, J. Phys. Chem. **94**, 4400 (1990).
[3] I.-W. Lyo and P. Avouris, Surf. Sci. **242**, 1 (1991).
[4] R. Martel, P. Avouris, and I.-W. Lyo, Science **272**, 385 (1996).
[5] C. Silvestre and M. Shayegan, Solid State Commun. **77**, 735 (1991).
[6] T. Miyake *et al.*, Phys. Rev. B **42**, 11 801 (1990).
[7] R. Kliese, B. Roettger, D. Badt, and H. Neddermeyer, Ultramicroscopy **42–44**, 824 (1992).
[8] P. Avouris and D. Cahill, Ultramicroscopy **42–44**, 838 (1992).
[9] H. W. Yeom, H. Hamamatsu, T. Ohta, and R. I. G. Uhrberg, Phys. Rev. B **59**, R10 413 (1999).
[10] B.-D. Yu *et al.*, Phys. Rev. B **70**, 033307 (2004).
[11] P. Avouris, I.-W. Lyo, and F. Bozso, J. Vac. Sci. Technol. B **9**, 424 (1991).
[12] G. Comtet, K. Bobrov, L. Hellner, and G. Dujardin, Phys. Rev. B **69**, 155315 (2004).
[13] H. Watanabe *et al.*, Phys. Rev. Lett. **80**, 345 (1998).
[14] K. Kato, T. Uda, and K. Terakura, Phys. Rev. Lett. **80**, 2000 (1998).
[15] T. Hoshino, M. Tsuda, S. Oikawa, and I. Ohdomari, Phys. Rev. B **50**, 14 999 (1994).
[16] T. Uchiyama and M. Tsukada, Phys. Rev. B **53**, 7917 (1996).
[17] D. J. Chadi, Phys. Rev. Lett. **59**, 1691 (1987).
[18] K. Hata, T. Kimura, S. Ozawa, and H. Shigekawa, J. Vac. Sci. Technol. A **18**, 1933 (2000).
[19] M. Nishizawa *et al.*, Phys. Rev. B **65**, 161302(R) (2002).
[20] T. Komura, T. Yao, and M. Yoshimura, Phys. Rev. B **56**, 3579 (1997).
[21] G. Kresse and J. Furthmuller, Phys. Rev. B **54**, 11 169 (1996).
[22] D. Vanderbilt, Phys. Rev. B **41**, R7892 (1990).
[23] The adsorption energy per an oxygen atom $E_{\mathrm{ad}}(X_n) = [E(X_n) - E(X_0) - nE_{\mathrm{O}}]/n$, where $E(X_n)$ is the total energy of the oxidation structure X_n, n the number of oxygen atoms in the unit cell, and E_{O} the spin-polarized total energy of a free oxygen atom.
[24] F. Matsui, H. W. Yeom, K. Amemiya, K. Tono, and T. Ohta, Phys. Rev. Lett. **85**, 630 (2000).
[25] K. Sakamoto, S. T. Jemander, G. V. Hansson, and R. I. G. Uhrberg, Phys. Rev. B **65**, 155305 (2002).
[26] B. A. Ferguson, C. T. Reeves, and C. B. Mullins, J. Chem. Phys. **110**, 11 574 (1999).
[27] J. M. Seo, K. J. Kim, H. W. Yeom, and C. Park, J. Vac. Sci. Technol. A **12**, 2255 (1994).
[28] X. L. Fan, Y. F. Zhang, W. M. Lau, and Z. F. Liu, Phys. Rev. Lett. **94**, 016101 (2005).